International Journal of Innovation Engineering and Technology Development
Vol.1, NO.1 , P:1 -11
Received: 20 December 2021
Accepted: 24 January 2022

L-lysine conjugated polymeric nanoparticles containing carbon dot for improving Idarubicin targeted delivery

Mahtab Amiri [1], Leila Hosseinzadeh [2] , Leila Behbood [2], Maryam Usefi [1], Abbas Hemati Azandaryani [1], Elham Arkan [1]*

*[*1] Nano Drug Delivery Research Center, Institute of Health Technology, Kermanshah University of Medical Sciences, Kermanshah, Iran.*
[2] Pharmaceutical sciences research center, Health Institute, Kermanshah University of Medical Sciences, Kermanshah, Iran

Abstract

Carbon dots as beneficial bioimaging agent, and hyaluronic acid as a biocompatible polymer with a potent affinity to bind cluster determinant 44, are extensively used in biomedical fields. In the present study, carbon dots were synthesized by the hydrothermal method from lemon juice, as a natural carbon source. Afterward, hyaluronic acid Nanoparticles, containing idarubicin and carbon dots were synthesized. The presence of carbon dots in the hyaluronic acid nanoparticles was confirmed by dependent photoluminescence spectroscopy and Fourier-transform infrared. Lysine was used on the surface of the hyaluronic acid nanoparticles as an essential amino acid with more willingness to enter the cancerous cells, which can be determinative in targeted drug delivery. The average size of the modified nanoparticles was 471± 23 nm and the measures showed uniform size distribution of hyaluronic acid nanoparticles. Lysine conjugation to nanoparticles was corroborated because the N-H peak around 3300 cm^{-1} in the spectrum of nanoparticles modified with Lysine was removed. The cytocompatibility of nanoparticles was proved by MTT assay. The results showed that nanoparticles conjugated with lysine containing idarubicin and carbon dots could be beneficial carriers for idarubicin against MCF-7 breast cancer cell line and carbon dots play an efficient role in these carriers as advantageous bioimaging agents.

Keyword: “Idarubicin, Polymeric Nanoparticles, Target Drug Delivery, Carbon Dots, Hyaluronic acid”

1. Introduction

Although many different kinds of traditional therapeutics have been used to treat various diseases such as cancers with some success, they caused many serious side effects, poor targeting, the possibility of occurring multidrug resistance (MDR) and rapid drug′s clearance. Moreover they cannot completely prevent the probability of relapse [1–7]. Nanomedicines come with a multitude number of benefits during recent years, including the ability of concurrent drug delivery, diagnosis and real-time tracking of chemotherapy efficacy, selective cancer-targeting ability, masked drug efficacy, etc. Moreover, they propose brilliant approaches to improve biodistribution and decrease toxicity and side effects of the drugs [8–14]. Recently, fluorescent nano-sized carbon dots (Cdots) have been suggested to present a wide variety of advantages. They have high chemical and optical stability, chemical inertness, excellent biocompatibility, low toxicity in comparison with traditional nanomaterials with high toxicity, low metabolic degradation, low photo-degradation, lack of blinking and high tunable photoluminescence (PL) properties (size- and excitation-wavelength (λ_{ex}) dependent photoluminescence (PL)) that make them superior to semiconductor quantum dots [15–20]. Cdots were discovered accidentally for the first time in the purification process of single-walled carbon nanotubes [21]. Top-down and

bottom-up methods ,as two main strategies, have been found to synthesize Cdots [22]. Top-down methods are including laser ablation method, arc-discharge and electrochemical oxidation and bottom-up methods are including thermal decomposition, combustion and microwave synthesis [23–25]. Since Cdots offer a great number of biochemical applications, they are highly used in drug delivery, photothermal therapy [22], bioimaging [26], contrast agent [27] and biosensor [28].

Hyaluronic acid (HA) is a biocompatible, cytocompatible, non-immunogenic and non-toxic natural polysaccharide in the body with a potent affinity to bind cluster determinant 44 (CD44), HA receptor for endocytosis (HARE) and lymphatic vessel endothelial Hyaluronic receptor (LYVE)-1, that are overexpressed on different kinds of tumor cells [29–33]. In the present study, HA-Cdots-lysine nanoparticles (NPs) loading with idarubicin (IDA), as an anthracyclin antitumor drug, which belongs to the family of drugs called antitumor antibiotics were synthesized. Furthermore, the cytotoxicity of the NPs on MCF-7 breast cancer cells was evaluated. HA-Cdots were used to bind to the related receptor cells (especially CD44 receptor cells) and also for labeling and imaging that specific kind of cells as fluorescent probes.

2. Materials and Methods

Idarubicin hydrochloride, dimethyl sulfoxide (DMSO), 1-ethyl-3-(3-dimethyl-aminopropyl) carbodiimide hydrochloride (EDS), N-Hydroxysuccinimide (NHS), L-lysine, sodium salt of hyaluronic acid with an M_w of 1000 KDa, and fetal bovine serum (FBS) were purchased from Sigma-Aldrich. Ammonium carbonate, potassium dihydrogen phosphate (KH_2PO_4), and acetone were obtained from Merck (Germany). All chemicals were utilized without any purification. Double distilled water was used for the following experiments.

2.1. Preparation of Carbon dots nanoparticles

Cdots were synthesized from lemon juice ,as a carbon source, using hydrothermal methods, as follows. Lemon juice was passed from a 2.5 µm membrane (a Whatman filter paper) to remove large particles. It was centrifuged for 15 min at 6000 rpm. Ammonium bicarbonate was solved in the juice. Then 10 ml of the clear pulp-free lemon juice was transferred into a 10 ml Teflon-lined stainless steel laboratory autoclave, and heated at 180°c for 7 hours. After the reaction was completed, the autoclave was cooled down to room temperature, naturally. The resulting suspension was centrifuged at 10000 rpm for 30 min and then the supernatant was further filtrated using a 0.2 µm membrane. Finally, the sample was freeze-dried and the dried powder form of Cdots was obtained (“Figure 1”).

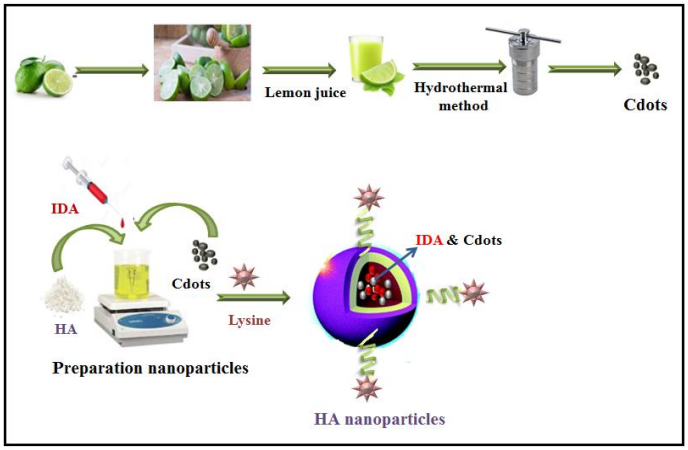

Figure 1. Schematic synthesis of Cdots from lemon juice and preparation of NPs containing IDA and Cdots

2.2. Preparation of conjugated NPs containing IDA and Cdots

The sodium salt of HA was solved in 10 ml phosphate buffer (pH= 5.5). 1 ml of Cdots suspension (45.52 mg/ml) and different concentrations of IDA in phosphate buffer (pH=5.5) were added drop wise to a fixed concentration of HA solution. The solution was sonicated on ice for 20 minutes using a bath sonication (Elmasonic, Germany). EDC and after that NHS were added to the solution to activate the carboxyl group. In the next step, the lysine was mixed to prepare conjugated NPs ("Figure 1"). It should be noted that Cdots, EDC and lysine were used with a molar ratio of 1:1 to HA. NHS was used with a molar ratio of 2:1 to HA and all of the solutions, including HA, Cdots, IDA, EDC, NHS and lysine solutions were prepared in phosphate buffer (pH= 5.5). Finally, the resulted NPs were freeze-dried.

2.3. Characterization of conjugated NPs

The size and zeta potential of NPs conjugated with lysine were analyzed using a zeta sizer (Malvern, Germany). The morphological characterization of the NPs was analyzed using a Transmission Electron Microscopy (TEM). The X-ray photoelectron patterns of HA, lysine, HA NPs and HA-lysine NPs were recorded for further verification of their various functional groups, using X-Ray Diffractometer (XRD) (Simens, Germany). Fluorescence emission and excitation spectra of Cdots with and without the ammonium bicarbonate conducted via various excitation wavelengths (from 200 to 600 nm), using Perkin–Elmer LS 45 Fluoro Spectrometer with a 10 mm quartz cuvette at room temperature. The FL WinLab Software (Perkin–Elmer) was applied for measurements and spectra recording. The instrument consists of two monochromators (excitation and emission), a Xenon light source, ranges of fixed-width selectable slits, selectable filters, attenuators and two photomultiplier tubes as detectors. The fluorimeter was connected to a PC microcomputer via an IEE serial interface. All measurements were performed in 10 mm quartz cells at room temperature. EEMs were registered in the ranges λ_{em} = 280–450 nm, each 0.5 nm, and λ_{ex} = 250–310 nm, each 2 nm. FT-IR analysis was done to investigate the presence of different polar functional groups on the surface of Cdots, HA, lysine and HA-Cdot-lysine NPs, using an FT-IR spectrophotometer (Irorestige-21, Shimadzu, China). The stability of the solutions was high for a long time without any aggregation or precipitation.

2.4. Encapsulation Efficiency (EE %)

After loading IDA to the HA NPs, the unbound IDA removed using dialysis for 12 h against phosphate buffer (pH=5.5). The external medium was renewed two times during dialysis. The IDA encapsulation Efficiency (EE) was evaluated by UV spectroscopy. The absorbance was detected at 255 nm using a UV spectrophotometer (MINI 1240, Shimadzu). Various concentrations of IDA were prepared and the UV absorptions were measured at 255 nm to obtain the calibration curve and calculate EE.

2.5. IDA release profile

To evaluate the release profile of IDA from the prepared NPs, 10 ml of the formulation was suspended in 1 ml phosphate buffer saline (PBS) (0.2 M, pH= 7.4) and was transferred into a dialysis bag (MWCO 12000 Da). Then it was placed in 30 ml PBS (0.2 M, pH= 7.4) in a shacking incubator at 37 °C. At specified intervals, 1 ml of solution from the outside release medium was removed and replaced with

1 ml of fresh buffer. The UV absorptions of the taken samples were measured at 470 nm. Thus, the amount of drug released could be calculated at different time intervals.

2.6. *In vitro* cytotoxicity

The cytotoxicity of the prepared formulations was investigated by a MTT assay method. A specific type of breast cancer cells (MCF-7 cell lines) was placed in each well of 96 well-plate at a density of 1.5×10^4 cells/well in the presence of RPMI 1640, supplemented with 10 % FBS and incubated in a humidified 5% CO_2-containing balanced air incubator (INC108, Memmert, Germany) at 37 °C for 24 h. Then the medium was replaced. Different concentrations of IDA in the form of HA NPs containing Cdots and IDA, and lysine conjugated HA NPs containing Cdot and IDA were added to the wells with three replicates and then incubated for 24 h. A group of cells was treated only with DMSO and considered as a control group. At predefined time intervals, the culture medium was replenished with MTT solution (0.5 mg/ml) and the plates were incubated at 37 °C for a further 3 h. Thereafter, DMSO (100 µl) was added to the each well to solubilize formazan crystals. Finally, the optical density of each well was evaluated at a test wavelength of 570 nm and a reference wavelength of 630 nm, using an Eliza microplate reader ((BioTek Instruments, USA). The viability of MCF-7 cells after exposure to different concentrations of nanoformulation was determined. All the MTT assays were conducted in triplicate and results were reported as Mean ± SEM in this study.

3. Results and Discussion

3.1. Preparation and characterization of Cdots, NPs containing Cdots and conjugated NPs containing IDA and Cdots

Natural products as useful sources were usually used in the synthesis of Cdots. In March 2018, Arkan and *et al* used walnut oil as a natural carbon precursor. They investigated and proved the apoptogenic and cytotoxic activities of the Cdots against PC3, MCF-7 and HT-29 human carcinoma cell lines [22]. In this study, Cdots were synthesized using lemon juice and ammonium bicarbonate as a nitrogen source to increase Cdots photoluminescence properties. Indeed, ammonium bicarbonate increases emission for a similar mass percentage of Cdots that proves the increased optical properties of Cdots for experimental and clinical studies. "Figure 2a and 2b" show the excitation and emission spectra of Cdots with and without ammonium bicarbonate. Cdots can be useful for multicolor bio-labeling and bio-imaging [34] and catalysis [35] due to their carboxyl and hydroxyl groups [36]. Moreover, several studies were done to show the anticancer properties of Cdots [37]. To characterize functional groups on the surface of HA, Cdots, lysine and conjugation formulation (HA-Cdot-lysine NPs) FT-IR evaluation was done ("Figure 3"). There is a significant peak around 3450 cm^{-1} on the FT-IR spectra of Cdots and HA-Cdot conjugates that demonstrates the presence of HA in the conjugates. The absence of C-N and C=O groups of Cdots on the FT-IR spectrum of HA-Cdot-lysine NPs indicates the presence of Cdots inside them. EDC and NHS activate the carboxylic group of HA and amine group of lysine and bind them to each other.

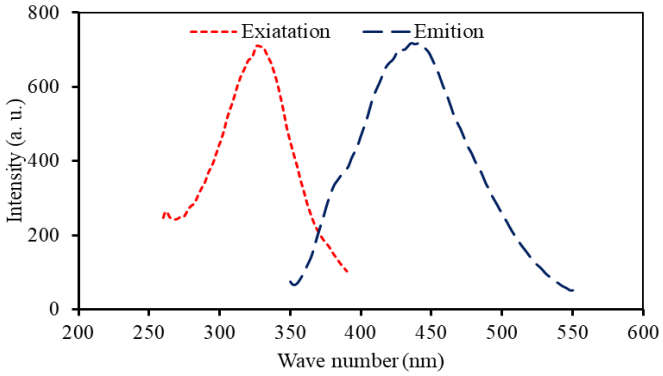

(a)

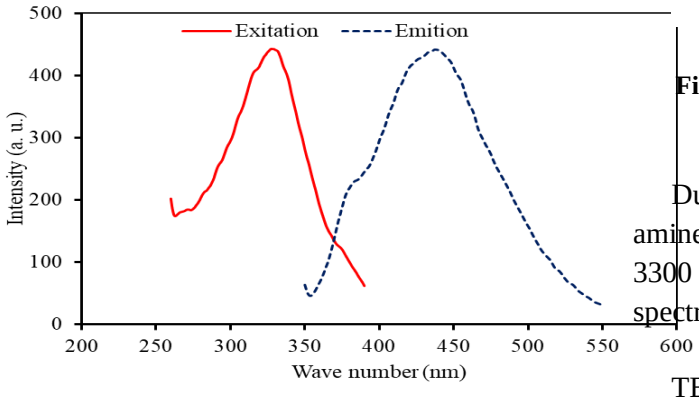

(b)

Figure 2. Emission and excitation spectra of cdots with (a) and without (b) ammonium bicarbonate

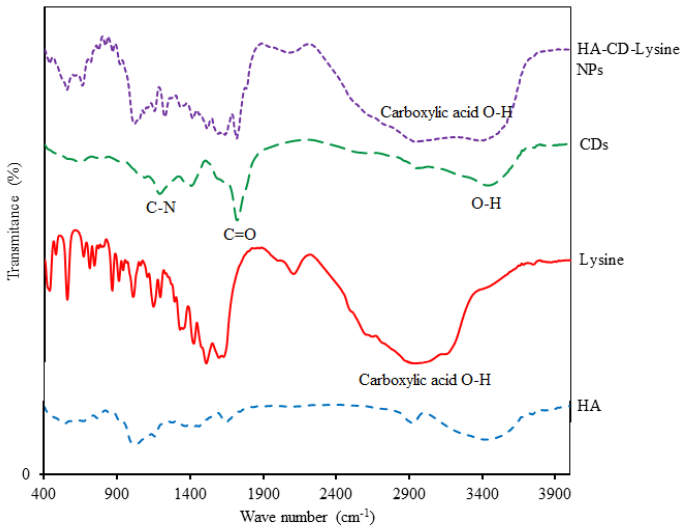

Figure 3. FT-IR spectra of HA, lysine, Cdots and HA-Cdot-lysine NPs

Due to the lysine, binding to HA via the amine group, the N-H peak of lysine around 3300 cm^{-1} removed in the HA-Ddot-lysine NPs spectrum.

TEM image was showed that the nanoparticles were spherical in shape ("Figure 4 A&B"). The particle sizes, determined by TEM were smaller than DLS measurements in "figure 5" because of sample preparation conditions: i.e., nanoparticles were prepared in a hydrated form for DLS measurements and in a dehydrated form for TEM images. Interestingly, the mean diameters of the nanoparticles exhibited no significant changes under physiological conditions (PBS, pH 7.4, 37 °C), over the period of seven days , explaining the nanoparticles are highly stable.

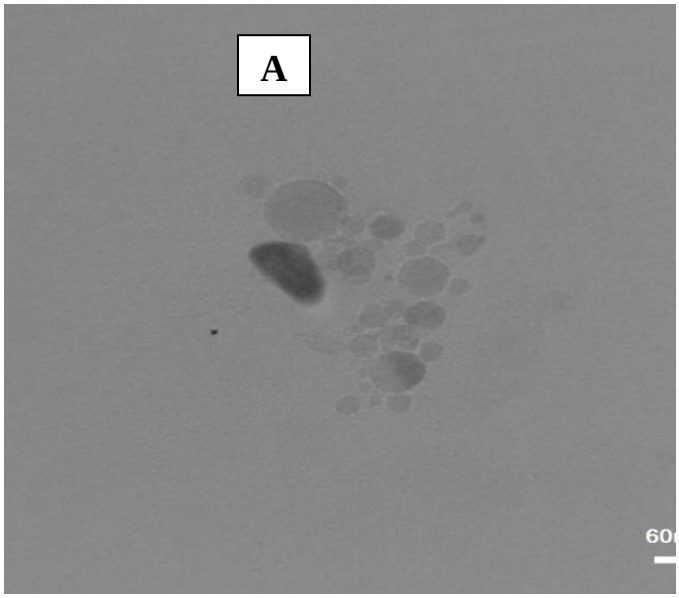

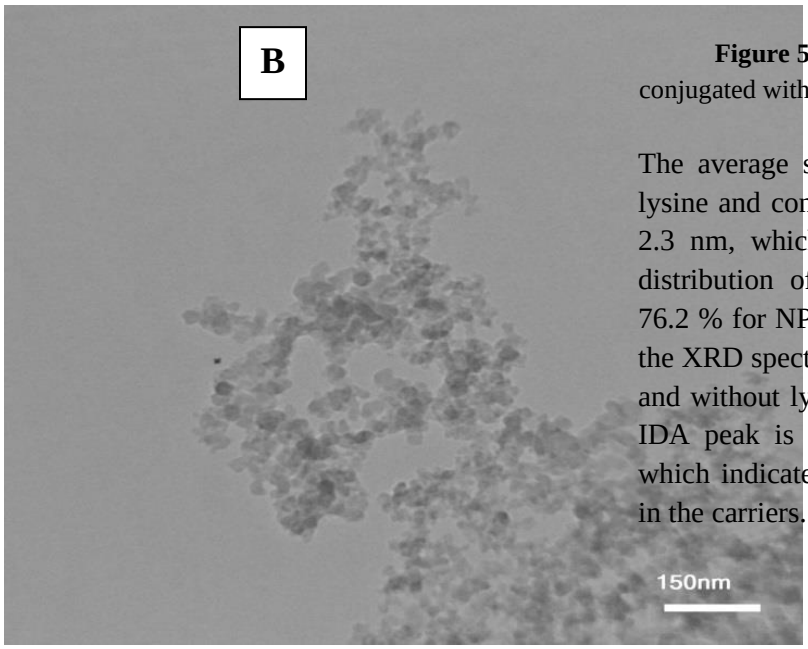

Figure 4 (A&B). TEM images of HA-Cdot-lysine NPs

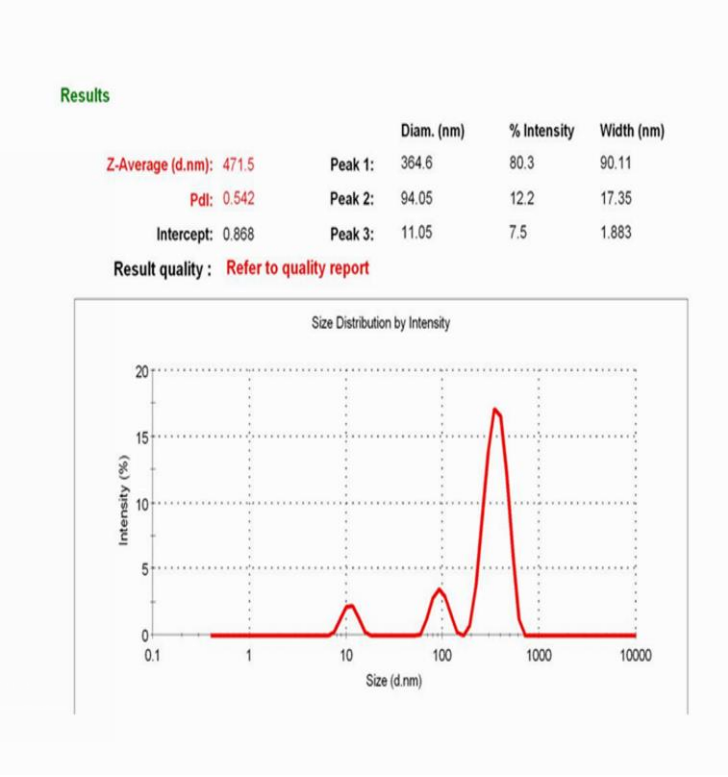

Figure 5. Average size and PdI of HA NPs conjugated with lysine and containing Cdots and IDA

The average size of HA NPs conjugated with lysine and containing Cdots and IDA was 471± 2.3 nm, which demonstrates the uniform size distribution of NPs. Entrapment efficiency of 76.2 % for NPs was obtained. “Figure 6” shows the XRD spectra of lysine and also HA NPs with and without lysine. As shown in this figure, the IDA peak is not observed in the NPs spectra which indicates amorphous loading of the drug in the carriers.

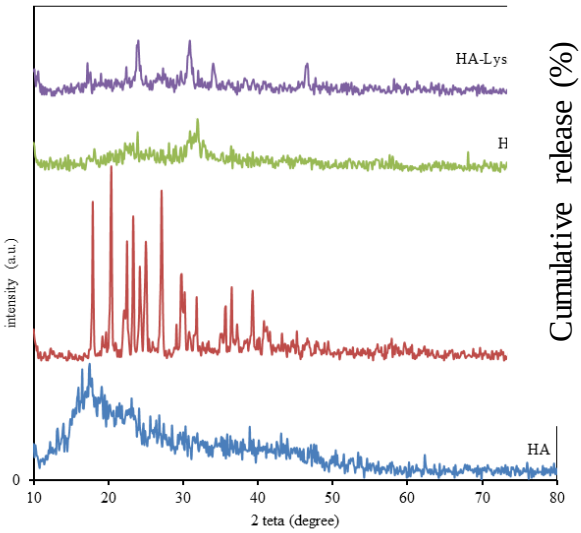

Figure 6. XRD spectra of HA, lysine, HA NPs and HA-lysine NPs

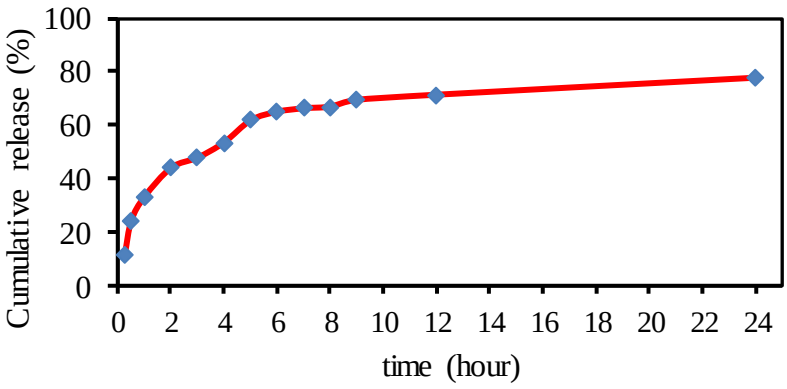

Figure 7. *In vitro* release profile of ID from HA-Cdot NPs

Rath and Pauling reported that lysine can inhibit ECM proteolysis and MMPs [38]. The anti-invasive and anti-proliferative potential of lysine were demonstrated on different human cancer cell lines. Cancerous cells have a higher affinity to lysine, as an essential amino acid, than normal cells. Conjugating HA NPs with lysine causes the increased entrance of nanocarriers into the cancerous cells [38].

3.2. IDA release profile

"Figure 7" shows *in vitro* release profile of IDA from HA-Cdot NPs. As shown in this figure, a burst release of 70 % was found within 9 h that increased to 78 % within 15 h under phosphate buffer at pH=5.5. The drug release was controlled after 9 h, which was due to the electrostatic interactions between the NP and the drug inside it. This controlled release profile of IDA can be helpful in counteracting cancerous tissues with mildly acidic environment.

3.3. *In vitro* cytotoxicity

In vitro cytotoxicity of different formulations against MCF-7 cells was examined. In order to examine the possible role of lysine in increasing cytotoxicity of IDA-loaded HA-Cdots NPs, two formulations (in the presence or absence of lysine) were compared in terms of cell viability. According to the results, conjugation of lysine to the formulation of HA-Cdots NPs potentiated the cytotoxicity of these NPs, leading to reduction of its IC_{50} from 0.056 to 0.039 mg/ml. These results altogether indicated the promising potential of nanoformulations including Cdots against MCF-7 cancer cells, which can be potentiated by conjugating lysine to Cdots ("Figure 8").

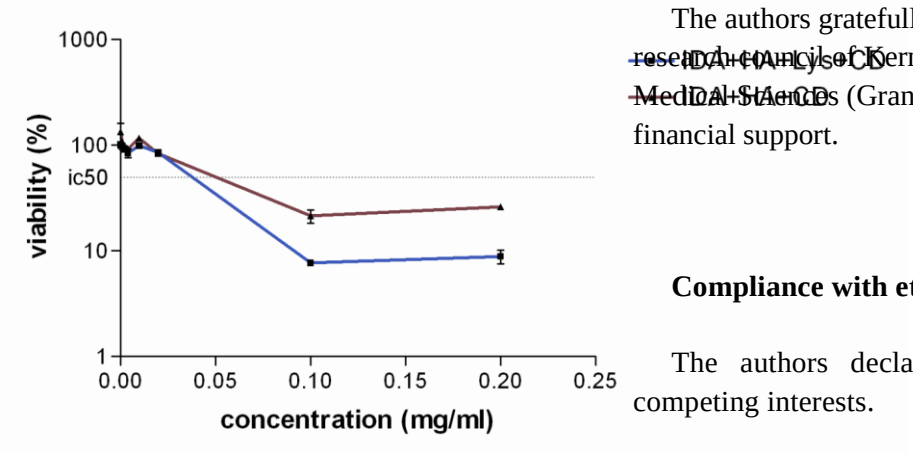

Figure 8. Cell viability percent of MCF-7 cells treated with different concentrations of IDA-loaded HA-CDs NPs with or without lysine

4. Conclusion

Cdots were synthesized from lemon juice, using hydrothermal methods, in presence of ammonium bicarbonate and confirmed by PL spectroscopy and FT-IR. HA-Cdot NPs were synthesized by amide bond formation between amine groups of Cdot and carboxylic groups of HA, which analyzed and confirmed by FT-IR. Lysine conjugation to HA-Cdot NPs was done and corroborated by FT-IR. The XRD test proved the amorphous drug loading inside the carrier. The average size of HA-Cdot-lysine NPs was 471± 2.3 nm and PdI was 0.5± 0.01. The cytocompatibility of IDA-loaded HA-Cdot-lysine NPs was proved by MTT assay. The current study represents lysine conjugated HA NPs containing carbon dot as a proper carrier of IDA against MCF-7 breast cancer cell line and Cdots as an advantageous bioimaging agent.

Acknowledgments

The authors gratefully acknowledge the research council of Kermanshah University of Medical Sciences (Grant Number. 96509) for financial support.

Compliance with ethical standards

The authors declare that they have no competing interests.

Conflict of interest

The authors declare that they have no conflict of interest.

References

[1] Zhang H., Wu H., Wang J., Yang Y., Wu D., Zhang Y., Zhang Y., Zhou Z., Yang S., (2015), Graphene oxide-BaGdF5 nanocomposites for multi-modal imaging and photothermal therapy. *Biomaterials*.42:66–77.

[2] Banik K., Harsha C., Bordoloi D., Lalduhsaki Sailo B., Sethi G., Leong HC., Arfuso F., Mishra S., Wang L., Kumar AP., Kunnumakkara AB., (2017), Therapeutic potential of gambogic acid, a caged xanthone, to target cancer. *Cancer Lett*. 416:75–86.

[3] Banik K., Sailo B., Thakur K., Jaiswal A., Javadi M., Bordoloi D., Kunnumakkara A., (2018), Potential of Different Chemosensitizers to Overcome Chemoresistance in Cervical Cancer. *Cancer Cell Chemoresistance And Chemosensitization*. p. 163–79.

[4] Javadi M., Jaiswal A., Banik K., Choudhary H., Singh A., Bordoloi D., Kunnumakkara A., (2018), Cancer Cell Chemoresistance: A Prime Obstacle in Cancer Therapy. C*ancer Cell Chemoresistance And Chemosensitization*. p. 15–49.

[5] Kunnumakkara AB., Bordoloi D., Harsha C., Banik K., Gupta SC., Aggarwal BB., (2017), Curcumin mediates anticancer effects by modulating multiple cell signaling pathways. *Clin. Sci. (Lond)*.131:1781–99.

[6] Padmavathi G., Roy NK., Bordoloi D., Arfuso F., Mishra S., Sethi G., Bishayee A., Kunnumakkara AB.,(2017), Butein in health and disease: A comprehensive review. *Phytomedicine*. 25:118–27.

[7] Begum S., Ahamed B., Ibrahim FB., Srinivasan H., (2021), Cancer nanomedicine : A review on approaches and applications towards targeted drug delivery. *Phytomedicine*. 12:310–27.

[8] Kumar R., Shin WS., Sunwoo K., Kim WY., Koo S., Bhuniya S., Kim J., (2015), Small conjugate-based theranostic agents: An encouraging approach for cancer therapy. *Chem. Soc. Rev*. 44:6670–83.

[9] Wu D., Si M., Xue H-Y., Wong H-L., (2017), Nanomedicine applications in the treatment of breast cancer: current state of the art. *Int. J. Nanomedicine*. 12:5879–92.

[10] Aulic S., Marson D., Laurini E., Fermeglia M., Pricl S., (2020), 16 - Breast cancer nanomedicine market update and other industrial perspectives of nanomedicine. Thorat ND, Bauer J, editors. *Nanomedicines for Breast Cancer Theranostics*. *Elsevier*. p. 371–404.

[11] Thorat N., Bauer J., (2020), Nanomedicine: next generation modality of breast cancer therapeutics. p. 1–14.

[12] Christianah Adebayo-Tayo B., Inem SA., Olaniyi OA., (2019), Rapid synthesis and characterization of Gold and Silver nanoparticles using exopolysaccharides and metabolites of Wesiella confusa as an antibacterial agent against Esherichia coli. *Int. J. Nano Dimens*. 10:37–47.

[13] Saadatmand MM., Yazdanshenas ME., Khajavi R., Mighani F., Toliyat T., (2019), Patterning the surface roughness of a nano fibrous scaffold for transdermal drug release. *Int. J. Nano Dimens*. 10:78–88.

[14] Verma P., Maheshwari SK., (2018), Applications of Silver nanoparticles in diverse sectors. I*nt. J. Nano Dimens*. 0(0).

[15] Yang ST., Wang X., Wang H., Lu F., Luo PG., Cao L., Meziani MJ., Liu JH., Liu Y., Chen M., Huang Y., Sun YP., (2009), Carbon dots as nontoxic and high-performance fluorescence imaging agents. *J. Phys. Chem. C*. 113:18110–4.

[16] Dong Y., Pang H., Yang HB., Guo C., Shao J., Chi Y., Li CM., Yu T., (2013), Carbon-based dots co-doped with nitrogen and sulfur for high quantum yield and excitation-independent emission. *Angew Chemie - Int. Ed*. 52:7800–4.

[17] Yan Y., Gong J., Chen J., Zeng Z., Huang W., Pu K., Liu J., Chen P., (2019), Recent Advances on Graphene Quantum Dots: From Chemistry and Physics to Applications. *Adv. Mater*. 31:1–22.

[18] Liu J., Geng Y., Li D., Yao H., Huo Z., Li Y., Zhang K., Zhu S., Wei H., Xu W., Jiang J., Yang B., (2020), Deep Red Emissive Carbonized Polymer Dots with Unprecedented Narrow Full Width at Half Maximum. *Adv. Mater*. 32:1–9.

[19] Zhang Z., Yi G., Li P, Zhang X., Fan H., Zhang Y., Wang X., Zhang C., (2020), A minireview on doped carbon dots for photocatalytic and electrocatalytic applications. *Nanoscale*. 12:13899–906.

[20] Yuan F., Wang Y-K., Sharma G., Dong Y., Zheng X., Li P., Johnston A., Bappi G., Fan JZ., Kung H., Chen B., Saidaminov MI., Singh K., Voznyy O., Bakr OM.,Lu ZH., Sargent EH., (2020), Bright high-colour-purity deep-blue carbon dot light-emitting diodes via efficient edge amination. *Nat. Photonics*. 14:171–6.

[21] Xu X., Ray R., Gu Y., Ploehn HJ., Gearheart L., Raker K., Scrivens W., (2004), Electrophoretic analysis and purification of fluorescent single-walled carbon nanotube fragments. *J. Am. Chem. Soc*. 126:12736–7.

[22] Liu C., Zhang P., Zhai X., Tian F., Li W., Yang J., Liu Y., Wang H., Wang W., Liu W., (2012), Nano-carrier for gene delivery and bioimaging based on carbon dots with PEI-passivation enhanced fluorescence. *Biomaterials*. 33:3604–13.

[23] Sun YP., Zhou B., Lin Y., Wang W., Fernando KAS., Pathak P., Meziani MJ., Harruff BA., Wang X., Wang H., Luo PG., Yang H., Kose ME., Chen B., Veca LM., Xie SY., (2006), Quantum-sized carbon dots for bright and colorful photoluminescence. *J. Am. Chem. Soc*. 128:7756–7.

[24] Liu H., Ye T., Mao C., (2007), Fluorescent carbon nanoparticles derived from candle soot. *Angew Chemie - Int. Ed*. 46:6473–5.

[25] Bourlinos AB., Stassinopoulos A., Anglos D., Zboril R., Karakassides M., Giannelis EP., (2008), Surface functionalized carbogenic quantum dots. *Small*. 4:455–8.

[26] Goh EJ., Kim KS., Kim YR., Jung HS., Beack S., Kong WH., Scarcelli G., Yun SH., Hahn SK., (2012), Bioimaging of hyaluronic acid derivatives using nanosized carbon dots. *Biomacromolecules*. 13:2554–61.

[27] Zhang M., Ju H., Zhang L., Sun M., Zhou Z., Dai Z., Zhang L., Gong A., Wu C., Du F., (2015), Engineering iodine-doped carbon dots as dual-modal probes for fluorescence and X-ray CT imaging. Int. J. *Nanomedicine*. 10:6943–53. [28] Tan L., He X., Chen D., Wu X., Li H., Ren X., Meng X.,Tang F., (2013), Highly H2O2-sensitive electrospun quantum dots nanocomposite films for fluorescent biosensor. *J. Biomed. Nanotechnol*. 9:53–60.

[29] Zhang M., Fang Z., Zhao X., Niu Y., Lou J., Zhao L., Wu Y., Zou S., Du F., Shao Q., (2016), Hyaluronic acid functionalized nitrogen-doped carbon quantum dots for targeted specific bioimaging. *RSC. Adv*. 6:104979–84.

[30] Tian H., Lin L., Chen J., Chen X., Park TG., Maruyama A., (2011), RGD targeting hyaluronic acid coating system for PEI-PBLG polycation gene carriers. *J. Control Release* 155:47–53. [31] Park JH., Cho HJ., Yoon HY., Yoon IS., Ko SH., Shim JS., Cho JH., Park JH., Kim K., Kwon IC., Kim DD., (2014), Hyaluronic acid derivative-coated

nanohybrid liposomes for cancer imaging and drug delivery. *J. Control Release*. 174(1):98–108.

[32] Sun C-Y., Zhang B-B., Zhou J-Y., (2019), Light-activated drug release from a hyaluronic acid targeted nanoconjugate for cancer therapy. *J. Mater Chem. B*. 7:4843–53.

[33] Wu P., Sun Y., Dong W., Zhou H., Guo S., Zhang L., Wang X., Wan M., Zong Y., (2019), Enhanced anti-tumor efficacy of hyaluronic acid modified nanocomposites combined with sonochemotherapy against subcutaneous and metastatic breast tumors. Nanoscale. 11(24):11470–83.

[34] Qu K., Wang J., Ren J., Qu X., (2013), Carbon dots prepared by hydrothermal treatment of dopamine as an effective fluorescent sensing platform for the label-free detection of iron(III) ions and dopamine. *Chem - A Eur. J*. 19:7243–9.

[35] Zhao S., Lan M., Zhu X., Xue H., Ng TW., Meng X., Lee CS., Wang P., Zhang W., (2015), Green Synthesis of Bifunctional Fluorescent Carbon Dots from Garlic for Cellular Imaging and Free Radical Scavenging. *ACS Appl. Mater Interfaces*. 7:17054–60.

[36] Yang C., Ogaki R., Hansen L., Kjems J., Teo BM., (2015), Theranostic carbon dots derived from garlic with efficient anti-oxidative effects towards macrophages. *RSC. Adv*. 5:97836–40.

[37] Li CL., Ou CM., Huang CC., Wu WC., Chen YP., Lin TE., Ho LC., Wang CW., Shih CC., Zhou HC., Lee YC., Tzeng WF., Chiou TJ., Chu ST., Cang J., Chang HT., (2014), Carbon dots prepared from ginger exhibiting efficient inhibition of human hepatocellular carcinoma cells. *J. Mater Chem*. B. 2:4564–71.

[38] Rath M., Pauling L., (1992), Plasmin-induced proteolysis and the role of apoprotein(a), lysine, and synthetic lysine analogs. *J. Orthomol Med*. 7:17–23.